Multi-track N-SBAS Sentinel-1 Interferometry focused on opencast mine monitoring: The case study of the Ptolemaida-Florina coal mine in Greece

Kleanthis Karamvasis[1], Vassilia Karathanassi[1]

[1] Laboratory of Remote Sensing, National Technical University of Athens, 9 Heroon Polytechniou Str., Zographos, Athens, Greece 15790 (karamvasisk@central.ntua.gr, karathan@survey.ntua.gr)

Key words: Deformation Monitoring; Sentinel-1; Small BAseline Subset (SBAS); Synthetic Aperture Radar Interferometry (InSAR); Ptolemaida-Florina coal mine

ABSTRACT

This paper illustrates the capabilities of distributed scatterer satellite Synthetic Aperture Radar Interferometry (InSAR) to monitor time-varying land deformation on mines. Due to continuous mining activities, monitoring ground deformation in and around mine areas has great importance to prevent possible slope instabilities that may lead to considerable casualties and cause several environmental issues. InSAR is considered a unique and well-established technique able to measure and monitor subtle surface displacements and deformation patterns over large areas. One of the main limitations of the aforementioned technique on the monitoring of opencast mining regions is the ambiguity of one dimensional line-of-sight measurements. In order to obtain insights on this limitation and optimally to transcend them, a multi-track Normalized Small Baseline Subset (N-SBAS) InSAR approach was applied. This technique is a modified SBAS approach that exploits the complementary information from multiple acquisition geometries of Sentinel-1 interferometric datasets. The combined use of ascending and descending Sentinel-1 geometries allowed to retrieve 3D deformation.

In this study, the open-pit coal mine located southern of town of Ptolemaida, Greece, has been successfully monitored by obtaining long-term time series ground displacement information. The study uses Sentinel-1 data collected over a period of 2.5 years (January 2016- June 2018). The estimated deformation was in accordance with field observations. The qualitative comparison of the produced results with ground measurements revealed the capabilities as well as the limitations of the proposed methodological approach. The results of this work indicate that the generated deformation maps can be a useful complementary data source for operational mining planning and risk assessment in the mining environment.

I. INTRODUCTION

Ground deformation information can be acquired from various techniques. Traditional ground-based methods such as leveling and GNSS (Global Navigation Satellite System) are widely used and considered the most accurate and well-developed methods (Colesanti et al., 2005). However, for extended areas, the aforementioned techniques are labor-intensive and limited in spatial coverage and density. By contrast, Multi-Temporal Synthetic Aperture Radar Interferometry (MT-InSAR) can obtain surface deformation along the line of sight (LOS) exploiting the phase information of the SAR images acquired at different times. A lot of MT-InSAR techniques have been developed and widely applied in many fields such as earthquake displacement (Massonnet et al., 1993; Biggs et al., 2009), volcanic activity (Massonnet et al., 1995; Papoutsis et al., 2013), groundwater/gas extraction (Chaussard et al., 2013), landslides instability (Calò et al., 2014; Zhao et al., 2016), urban subsidence (Osmanoğlu et al., 2011), and mining activity (Samsonov et al., 2013).

MT-InSAR techniques were proven to be powerful tools and have gained increasing attention because they can provide at all-times, all-weather deformation information in a wide area. The latter is related with the recent advances in terms of the temporal/spatial resolution and coverage of satellite data, the processing chains and the increase of the computational capabilities (parallel processing, cloud computing) (Raspini et al., 2018). A brief summary of the most important MT-InSAR methods is presented in the next paragraph.

The first MT-InSAR approach named Persistent Scatterers Interferometry (PSI) was firstly introduced by Ferretti et al., 2000 which estimates the deformation only at points that have high amplitude dispersion index. The next step was the Small BAseline Subset (SBAS) approach from Berardino et al., 2002 which exploits the information only from the interferograms with low spatial decorrelation that is translated to relatively small baselines. SBAS approaches improves the spatial density of the measurement points by extracting information from the distributed scatterers. The next algorithmic improvement was related with the loosening of the restrictive conditions imposed by the

PSI by exploiting the coherence information. Coherent Pixel technique (Wu et al., 2008) and Partially Coherent Target technique (P-CT) (Perissin & Wang 2012) are the most representative examples. Lastly, methodologies that combine the information from persistent and distributed scatterer methods have been introduced (Hooper et al., 2008, Ferretti et al., 2011). The main drawback of the latter methods is their computational efficiency using large-archives of SAR data especially for large-scale areas (Ferretti et al., 2011). It is important to state that in each application, each algorithm possesses inherently unique strengths and weaknesses due to specific characteristics in each case (Osmanoğlu et al., 2016).

Deformation monitoring in mining areas has a great importance because mining activities impact the nearby environment and may cause severe mining hazards (Loupasakis et al., 2014). From the "interferometric" point of view, the mining areas have some special issues that have to be addressed. First of all, it is the loss of coherence that is usually caused by the mining operations that prevent the detection of ground surface deformation (Raucoules et al., 2007). Secondly, the low density and the inhomogeneous distribution of persistent scatterers in the mining regions limit the use of high-accurate persistent scatterer methods (Jung et al., 2007; Yue et al., 2011). In contrast, SBAS techniques allow the measurement of surface displacements in low reflectivity areas like scattered outcrops, bare soil areas, debris areas that are usually found in mining regions (Liu et al., 2014).

In this paper, a Sentinel-1 multi-track methodology based on N-SBAS (Doin et al., 2011) is presented. The main objective of this study is to explore the deformation monitoring ability of the proposed methodology in mining regions. The case study of the Ptolemaida-Florina coal mine in Greece helped us to outline the strengths and the limitations of the proposed methodology. Validation between multi-track N-SBAS and levelling measurements was conducted. The output of this study shows the effectiveness of the Sentinel-1 constellation for the monitoring of ground subsidence over non-active mining areas. Moreover the results can be useful for management, risk analysis and planning of mining operations.

II. Methodology

The proposed methodology contains four processing steps. The first step is related to the interferometric processing of SAR data from a track and the production of a geocoded single-track interferometric stack. The first step is performed for an ascending and a descending track. As a second step the preprocessing of each interferometric stack is performed. The third step is related to the time-series analysis of the single-track interferometric stack and the inversion in order to obtain deformation values. Finally the fourth step includes the combination of the available deformation information obtained by the two different tracks in order to extract vertical, easting and northing deformation.

A. *Interferometric processing*

For the interferometric processing the Interferometric SAR Scientific Computing Environment (ISCE) (Rosen et al., 2012) has been used. The interferometric workflow starts with a number of Sentinel-1A/B Interferometric Wide Swath (IW) mode Single Look Complex (SLC) acquisitions. According to the user`s criteria a network of viable differential interferograms is created. The criteria are related with the spatial and temporal baseline of the interferograms. Then, the main steps of the interferometric processing such as, orbit correction, deburst, co-registration, interferogram generation and adaptive filtering, subtraction of topographic phase using given Digital Elevation Model (DEM), unwrapping and geocoding are implemented. It`s important to state, that each interferogram was calculated independently and geocoded in a common geographical grid. A batching process was developed based on (Henderson, 2018).

B. *Preprocessing of geocoded interferometric stacks*

In this step, each stack is prepared in a consistent way to further be processed. The main preparation processes were implemented based on GIAnT software package scripts (Agram et al., 2012; Agram et al., 2013). The first step is related with the mitigation of the unwrapping errors based on (Pinel-Puysségur et al., 2018) with the assumption that the SAR phase field is conservative (Biggs et al., 2007). The second sub-step is the correction of the residual orbital errors by network deramping. Firstly, for each interferogram a ramp is estimated and then a best ramp for all the interferometric stack is re-estimated and removed (Biggs et al., 2007; Jolivet et al., 2012). As a final sub-step, the network of interferograms was corrected from the atmospheric effects due to the propagation delays of the SAR signal. The correction approach was based on a multiscale approach that estimates topographically correlated atmospheric delays (Lin et al., 2010).

C. *Time series analysis/Inversion*

The third processing step is a time series analysis which was applied separately per each geocoded interferometric stack. The N-SBAS inversion technique implemented in GIAnT software package was employed. The inversion technique was performed in each pixel separately subject to coherence and valid number of observation criteria. The main difference of

N-SBAS with respect to the conventional SBAS technique (Berardino et al., 2002) is that it includes quadratic constraints to join clusters of disconnected interferograms. A detailed description of N-SBAS inversion technique can be found in López-Quiroz et al., 2009; Doin et al., 2011; Jolivet el al., 2012.

D. *Integration of Multi-track deformations*

One of the limitations of deformation measurements made with MT-InSAR techniques is that they provide only one component of the surface deformation—in the satellite's line of sight (LOS) (Wright et al., 2004). The availability of ascending and descending tracks of Sentinel-1 constellation that cover the same region is important in order to resolve the 3D surface deformation. As we already stated, for each pixel in each geometry/track we can have only one deformation measurement along LOS which can be decomposed to northing, easting and vertical components (Figure 1).

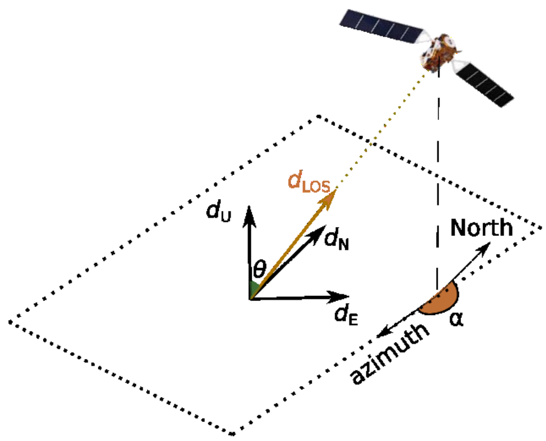

Figure 1 The SAR imaging geometry and the relationship between LOS deformation and the vertical, North-South and East-West components. θ and α are the radar incidence angle and the orbit azimuth angle, respectively.

According to Figure 1, the following equation derives (Wright et al., 2004; Hu et al., 2010):

$$d_{LOS} = d_U cos\theta + d_N sin\alpha sin\theta + d_E cos\alpha cos\theta \; (1)$$

Where d_{LOS} = deformation along LOS

d_U, d_N, d_E = Vertical, North-South, East-West deformation components

α = heading angle

θ = incidence angle

From a theoretical point of view, in order to be able to resolve the 3D deformation components we need at least three LOS deformation measurements. Due to high computational cost to obtain deformation time series for three tracks we propose the following method.

The main assumption of the method is that a part of the neighborhood pixels share the same deformation behavior with the central pixel for which we want to obtain the 3D deformation components. The neighborhood pixels are defined by a 3x3 window. The gradient is the criterion for neighborhood pixel selection. Gradient is estimated using a DEM with better resolution than the SAR grid. Neighborhood pixels with similar gradient with the central pixel are selected for the solution of system of equations (1). In the following section a case study in Ptolemaida-Florina mine is presented.

III. Area of Interest and Data

The area of interest is located in the region of Western Macedonia (Kozani), Greece, which is considered one of the most important industrial areas in Greece. In particular this work focuses on a part of the Ptolemaida-Florina opencast lignite mine, illustrated in the left part of Figure 2.

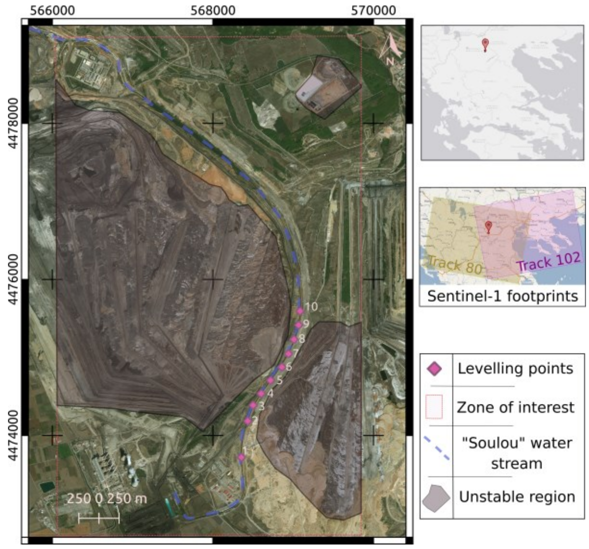

Figure 2 Study area (part of Ptolemaida-Florina coal mine) and available datasets (Sentinel-1 and levelling). Reference system is WGS84 UTM34N. The background image is a very high resolution optical image © Google Earth Copyright 2018.

Due to the mining activities in the zone of interest "unstable" regions were delineated. In Figure 2, the "unstable" regions are denoted with a gray color. In these regions, MT-InSAR technique cannot provide reliable results due to strong decorrelation of the SAR signal. The main objective of the case study is to examine the stability of the zone along "Soulou" water stream that could potentially provide insight about the risks of the existing transportation network inside the mining area. For the validation of the results of the proposed methodology 10 leveling points located in the buffering zone along the "Soulou" water stream have been used.

A total of 249 Sentinel-1 TOPS IW acquisitions from the descending track 80 and the ascending track 102, spanning two and a half years have been processed. Around 1400 interferograms were created and processed with the multi-track N-SBAS technique that was described in the previous section. The processed area is about 4x8 km^2. The earlier scene of each orbit stack was selected as the zero-deformation reference image. As an external DEM, we used a photogrammetric DEM with ground pixel size of 5 m, provided by KTIMATOLOGIO S.A.

IV. Results and Validation

In this section the most significant results are reported and analyzed. In Figure 3 the cumulative displacements for the time period from the start of 2016 till the half of 2018 are presented. It`s important to state that these results are relative with respect to the first acquisition date of 2016, which we used as a zero-displacement reference. The pixel size of each map/grid in Figure 3 per each component is 15m.

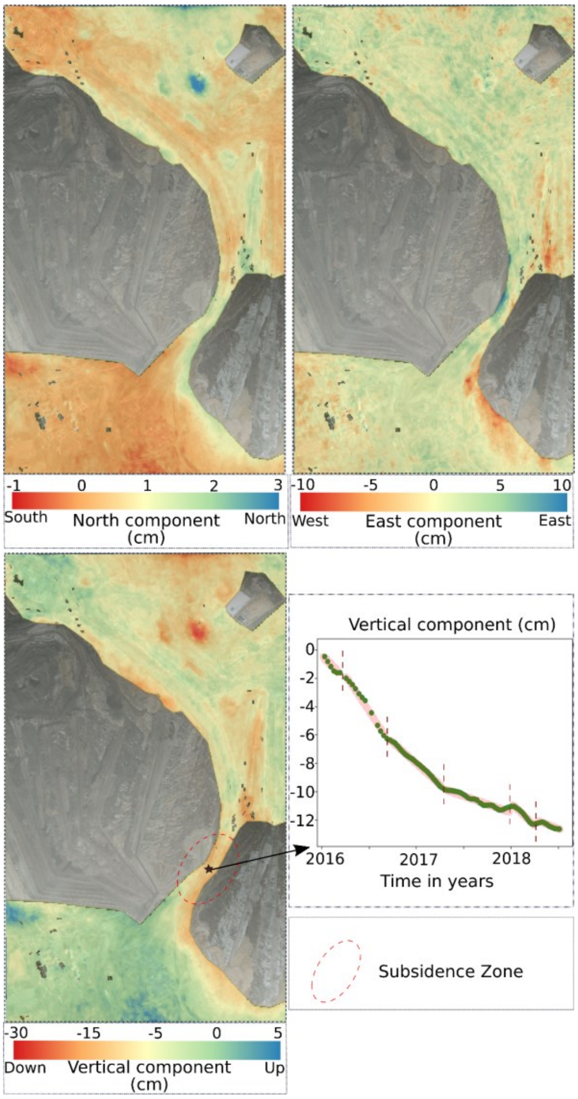

Figure 3 Cumulative displacement components from 10/1/2016 to 5/7/2018. Time series of displacement inside the subsidence zone (bottom right).

We can easily identify that the vertical displacement values are relatively higher than in the other directions. Looking closely at the vertical component we can also identify the subsidence zone (red ellipse) possibly because of the vicinity with the active mining regions (gray regions).

It`s important to state that for each point in the grid the time series of displacement are calculated. Inside the subsidence zone, the time series displacement information of a point (bottom right of Figure 3) is presented. Different linear components of the deformation in a time sense can be identified. The decreasing behavior of the subsidence rates is clearly showed evident.

The validation procedure has been performed by comparing the vertical component of multi-track N-SBAS approach with the levelling measurements in the levelling points (Figure 2) close to the subsidence zone. The overall root mean square error between all the leveling measurements (160) at 10 leveling points and the multi-track N-SBAS estimations is 1.07 cm.

In Figure 4, for each point, the evolution of the subsidence according to leveling measurements and to multi-track N-SBAS estimations (denoted as SAR estimations) is presented. In most cases, SAR estimations tend to overestimate subsidence values. On the other hand, the subsidence rates between the two different methods are in good agreement. The analysis of the results show that centimetric accuracy can be achieved with the proposed technique when monitoring subsidence in a complex mining environment.

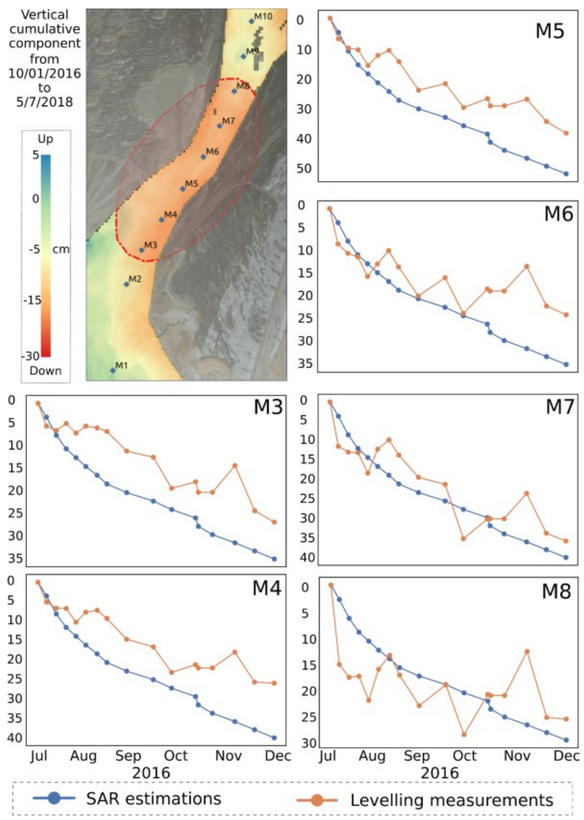

Figure 4 Time series of vertical ground deformations for six locations in the subsidence region. The nearest centroid of the deformation grid was selected according to location of the leveling point. Values in diagrams are related with subsidence and expressed in mm.

V. Discussion

The above results demonstrate that the subsidence zone along a part of the "Soulou" water stream can be identified by the proposed methodology. The regional subsidence as well the subsiding trend could be adequately estimated. The subsidence is possibly connected with operations in the mine. However, the interpretation of the measured/observed deformation patterns is a complex task and requires the knowledge of the geological, tectonic, hydrogeological and geotechnical conditions. A deeper understanding of the subsidence mechanism requires more investigation.

The validation of the methodology for average subsidence and subsidence rates showed that the proposed method is able to provide high temporal/ spatial resolution and accurate subsidence information. In other studies such as Ferretti et al., 2011, millimetric accuracy level has been achieved using an approach mainly based on persistent scatterer interferometry. Due to the absence of persistent scatterers in the study area, the centimetric level of accuracy is considered satisfactory. Combining InSAR and leveling measurements can be a good strategy to better monitor the subsidence of the area of interest. One possible solution for better monitoring of the subsidence phenomena could be the following: (1) to detect the hotspot areas using the multi-track N-SBAS technique over the whole region; and (2) to plan ground survey measurements and collect precise ground information about the hotspot areas.

One of the most important limitation of the proposed method is related with the orientation and the slope of the ground. In steep-slope regions, the reliability of the interferometric estimations is decreased mainly due to geometric distortions of the SAR signal (Colesanti et al. 2005). The geometric distortions also affect the spatial resolution of the SAR sensor which will cause lower spatial resolution of the final deformation results.

Another limitation factor of the proposed method is the 1- dimensional measurement of SAR systems in the LOS direction (Wright et al., 2004). Moreover, due to the current near-polar orbiting SAR sensors the accuracy of each estimated component is different. The north component is considered the most difficult to determine, due to the small angular separation of the different LOSs (Wright et al., 2004).

In other studies, 3D deformations have been resolved using offset-tracking azimuth techniques (Strozzi et al., 2002; Yang et al., 2018) and multi-aperture InSAR techniques (Hu et al., 2012; Jung et al., 2011). The aforementioned techniques are valuable tools mainly in studies of large-scale displacement events like earthquakes, volcano eruption, glacier dynamics but they cannot provide sufficient accuracy for small-scale deformation phenomena (Hu et al., 2014). The proposed approach which is based on the combination of multiple track interferometric results produces estimations with sufficient accuracy at the vertical direction (centimetric level). Even though a lot of methods that resolve the 3D deformation components have been developed, it remains unclear which approach is the most suitable for each case (Hu et al., 2014).

One of the benefits of the proposed method is that the produced results can support decision makers for mining risk management and disaster awareness. The fact is that active mining operations are well monitored by the mining authorities. However in abandoned mines or abandoned regions of the mines even though they have been considered secured, hidden factors can cause geohazards at any time (Benecke et al. 2012). The proposed method can provide critical information to mitigate fatalities and ensure the safety of mining operations and local societies during pre-mining, mining and post-mining period.

VI. Conclusions

The multi-track N-SBAS InSAR method yielded deformation results with centimetric level of accuracy at the vertical component. It has to be tested in regions with different conditions and to be compared with other methods. The results of the proposed method can be used for further planning of the ground surveys from mine authorities. Using Sentinel-1 free data the proposed method can provide regional coverage and continuous delivery information with no cost. We believe that the produced results can support decision making authorities for risk mitigation and sustainability.

VII. Acknowledgements

We would like to thank the European Space Agency (ESA) for supplying the Sentinel-1 images. The authors would like to acknowledge KTIMATOLOGIO S.A. for kindly providing the DEM for the study area and the Mines Central Support Department of Public Power Corporation S.A.-Hellas for kindly providing the levelling data. The authors would also like to thank the anonymous reviewers for their contribution to the improvement of the overall quality of the manuscript. Finally we would like to thank UNAVCO Inc., Caltech and JPL for the ISCE and GIAnT software packages.

References

Agram, P. S., Jolivet, R., Riel, B., Lin, Y. N., Simons, M., Hetland, E., ... & Lasserre, C. (2013). New radar interferometric time series analysis toolbox released. *Eos, Transactions American Geophysical Union*, 94(7), 69-70.

Agram, P., Jolivet R. and Simons, M., Generic InSAR Analysis Toolbox (GIAnT) - *User Guide* (2012), http://earthdef.caltech.edu.

Benecke N, Zimmermann K, Marsh S (leading authors) (2012) Perspectives concerning satellite EO andgeohazard risk management: inactive mine hazards. In: *Bally Ph (ed)*

Scientific and technical mem-orandum of the international forum on satellite EO and geohazards, 21–23 May 2012, Santorini Greece, European Space Agency. doi:10.5270/esa-geo-hzrd-2012.

Berardino, P., Lanari, R. and Sansosti, E., 2002, A new algorithm for surface deformation monitoring based on small baseline differential SAR interferograms. *IEEE Transactions on Geoscience and Remote Sensing*, 40, 2375−2383 p.

Biggs, J., Wright, T., Lu, Z., & Parsons, B. (2007). Multi-interferogram method for measuring interseismic deformation: Denali Fault, Alaska. *Geophysical Journal International,* 170(3), 1165-1179.

Biggs, J.; Bürgmann, R.; Freymueller, J.T.; Lu, Z.; Parsons, B.; Ryder, I.; Schmalzle, G.; Wright, T. The postseismic response to the 2002 M 7.9 Denali Fault earthquake: Constraints from InSAR 2003–2005. *Geophysical Journal International*. 2009, 176, 353–367.

Calò, F.; Arizzone, F.; Castaldo, R.; Lollino, P.; Tizzani, P.; Guzzetti, F.; Lanari, R.; Angeli, M.; Pontoni, F. Manunta, M. Enhanced landslide investigation through advanced DInSAR techniques: The Ivancich case study, Assisi, Italy. *Remote Sensing of Environment*. 2014, 142, 69–82.

Chaussard, E., Amelung, F., Abidin, H., & Hong, S. H. (2013). Sinking cities in Indonesia: ALOS PALSAR detects rapid subsidence due to groundwater and gas extraction. *Remote Sensing of Environment*, 128, 150-161.

Colesanti, C., Mouelic, S. L., Bennani, M., Raucoules, D., Carnec, C., & Ferretti, A. (2005). Detection of mining related ground instabilities using the Permanent Scatterers technique—a case study in the east of France. *International Journal of Remote Sensing*, 26(1), 201-207.

Doin, M. P., Guillaso, S., Jolivet, R., Lasserre, C., Lodge, F., Ducret, G., & Grandin, R. (2011, September). Presentation of the small baseline NSBAS processing chain on a case example: The Etna deformation monitoring from 2003 to 2010 using Envisat data. *In Proceedings of the Fringe Symposium* (pp. 3434-3437). ES.

Ferretti, A., Prati, C., & Rocca, F. (2001). Permanent scatterers in SAR interferometry. *IEEE Transactions on geoscience and remote sensing*, 39(1), 8-20.

Ferretti, A., Fumagalli, A., Novali, F., Prati, C., Rocca, F., & Rucci, A. (2011). A new algorithm for processing interferometric data-stacks: SqueeSAR. *IEEE Transactions on Geoscience and Remote Sensing*, 49(9), 3460-3470.

Henderson, S. (2018). Tools for ISCE (InSAR Scientific Computing Environment) *GitHub repository*, https://github.com/scottyhq/isce_notes

Hooper, A. (2008). A multi-temporal InSAR method incorporating both persistent scatterer and small baseline approaches. *Geophysical Research Letters*, 35(16).

Hu, J., Li, Z., Zhu, J., Ren, X., & Ding, X. (2010). Inferring three-dimensional surface displacement field by combining SAR interferometric phase and amplitude information of ascending and descending orbits. *Science China Earth Sciences*, 53(4), 550-560.

Hu, J., Li, Z. W., Ding, X. L., Zhu, J. J., Zhang, L., & Sun, Q. (2012). 3D coseismic displacement of 2010 Darfield, New Zealand earthquake estimated from multi-aperture InSAR and D-InSAR measurements. *Journal of Geodesy*, 86(11), 1029-1041.

Hu, J., Li, Z. W., Ding, X. L., Zhu, J. J., Zhang, L., & Sun, Q. (2014). Resolving three-dimensional surface displacements from InSAR measurements: A review. *Earth-Science Reviews*, 133, 1-17.

Jolivet, R., Lasserre, C., Doin, M. P., Guillaso, S., Peltzer, G., Dailu, R., ... & Xu, X. (2012). Shallow creep on the Haiyuan fault (Gansu, China) revealed by SAR interferometry. *Journal of Geophysical Research: Solid Earth,* 117(B6).

Jung, H. C., Kim, S. W., Jung, H. S., Min, K. D., & Won, J. S. (2007). Satellite observation of coal mining subsidence by persistent scatterer analysis. *Engineering Geology*, 92(1-2), 1-13.

Jung, H. S., Lu, Z., Won, J. S., Poland, M. P., & Miklius, A. (2011). Mapping three-dimensional surface deformation by combining multiple-aperture interferometry and conventional interferometry: Application to the June 2007 eruption of Kilauea volcano, Hawaii. *IEEE Geoscience and Remote Sensing Letters*, 8(1), 34-38.

Lin, Y. N. N., Simons, M., Hetland, E. A., Muse, P., & DiCaprio, C. (2010). A multiscale approach to estimating topographically correlated propagation delays in radar interferograms. *Geochemistry, Geophysics, Geosystems*, 11(9).

Liu, D., Shao, Y., Liu, Z., Riedel, B., Sowter, A., Niemeier, W., & Bian, Z. (2014). Evaluation of InSAR and TomoSAR for monitoring deformations caused by mining in a mountainous area with high resolution satellite-based SAR. *Remote Sensing*, 6(2), 1476-1495.

López-Quiroz, P., Doin, M. P., Tupin, F., Briole, P., & Nicolas, J. M. (2009). Time series analysis of Mexico City subsidence constrained by radar interferometry. *Journal of Applied Geophysics*, 69(1), 1-15.

Loupasakis, C., Angelitsa, V., Rozos, D., & Spanou, N. (2014). Mining geohazards—land subsidence caused by the dewatering of opencast coal mines: The case study of the Amyntaio coal mine, Florina, Greece. *Natural hazards*, 70(1), 675-691.

Massonnet, D.; Rossi, M.; Carmona, C.; Adragna, F.; Peltzer, G.; Feigl, K.; Rabaute, T. The displacement field of the Landers earthquake mapped by Radar interferometry. *Nature* 1993, 364, 138–142.

Massonnet, D.; Briole, P.; Arnaud, A. Deflation of Mount Etna monitored by spaceborne Radar interferometry. *Nature* 1995, 375, 567–570

Osmanoğlu, B., Dixon, T. H., Wdowinski, S., Cabral-Cano, E., & Jiang, Y. (2011). Mexico City subsidence observed with persistent scatterer InSAR. *International Journal of Applied Earth Observation and Geoinformation*, 13(1), 1-12.

Osmanoğlu, B., Sunar, F., Wdowinski, S., & Cabral-Cano, E. (2016). Time series analysis of InSAR data: Methods and trends. *ISPRS Journal of Photogrammetry and Remote Sensing*, 115, 90-102.

Papoutsis, I., Papanikolaou, X., Floyd, M., Ji, K. H., Kontoes, C., Paradissis, D., & Zacharis, V. (2013). Mapping inflation at Santorini volcano, Greece, using GPS and InSAR. *Geophysical Research Letters*, 40(2), 267-272.

Perissin, D., & Wang, T. (2012). Repeat-pass SAR interferometry with partially coherent targets. *IEEE*

Transactions on Geoscience and Remote Sensing, 50(1), 271-280.

Pinel-Puysségur, B., Lasserre, C., Benoit, A., Jolivet, R., Doin, M. P., & Champenois, J. (2018, July). A Simple Phase Unwrapping Errors Correction Algorithm Based on Phase Closure Analysis. In *IGARSS 2018-2018 IEEE International Geoscience and Remote Sensing Symposium* (pp. 2212-2215). IEEE.

Raspini, F., Bianchini, S., Ciampalini, A., Del Soldato, M., Solari, L., Novali, F., ... & Casagli, N. (2018). Continuous, semi-automatic monitoring of ground deformation using Sentinel-1 satellites. *Scientific reports*, 8.

Raucoules, D., Colesanti, C., & Carnec, C. (2007). Use of SAR interferometry for detecting and assessing ground subsidence. *Comptes Rendus Geoscience*, 339(5), 289-302.

Rosen, P. A., Gurrola, E., Sacco, G. F., & Zebker, H. (2012, April). The InSAR scientific computing environment. *In Synthetic Aperture Radar, 2012. EUSAR. 9th European Conference* on (pp. 730-733). VDE.

Samsonov, S., d'Oreye, N., & Smets, B. (2013). Ground deformation associated with post-mining activity at the French–German border revealed by novel InSAR time series method. *International Journal of Applied Earth Observation and Geoinformation*, 23, 142-154.

Strozzi, T., Luckman, A., Murray, T., Wegmuller, U., & Werner, C. L. (2002). Glacier motion estimation using SAR offset-tracking procedures. *IEEE Transactions on Geoscience and Remote Sensing*, 40(11), 2384-2391.

Wright, T. J., Parsons, B. E., & Lu, Z. (2004). Toward mapping surface deformation in three dimensions using InSAR. *Geophysical Research Letters*, 31(1).

Yang, Z., Li, Z., Zhu, J., Preusse, A., Hu, J., Feng, G., & Papst, M. (2018). Time-Series 3-D Mining-Induced Large Displacement Modeling and Robust Estimation From a Single-Geometry SAR Amplitude Data Set. *IEEE Transactions on Geoscience and Remote Sensing.*

Yue, H., Liu, G., Guo, H., Li, X., Kang, Z., Wang, R., & Zhong, X. (2011). Coal mining induced land subsidence monitoring using multiband spaceborne differential interferometric synthetic aperture radar data. *Journal of Applied Remote Sensing*, 5(1), 053518.

Zhao, C., Zhang, Q., He, Y., Peng, J., Yang, C., & Kang, Y. (2016). Small-scale loess landslide monitoring with small baseline subsets interferometric synthetic aperture radar technique—case study of Xingyuan landslide, Shaanxi, China. *Journal of Applied Remote Sensing,* 10(2), 026030.